REPORT DOCUMENTATION PAGE

1

Form Approved OMB NO. 0704-0188

1. REPORT DATE (DD-MM-YYYY)	2. REPORT TYPE	3. DATES COVERED (From - To)
31-08-2014	Manuscript	-

4. TITLE AND SUBTITLE
Size Dependent Mechanical Behavior of Free-Standing Glassy Polymer Thin Films

5a. CONTRACT NUMBER
W911NF-13-1-0241

5b. GRANT NUMBER

5c. PROGRAM ELEMENT NUMBER
611102

6. AUTHORS
Wenjie Xia , Sinan Keten

5d. PROJECT NUMBER

5e. TASK NUMBER

5f. WORK UNIT NUMBER

7. PERFORMING ORGANIZATION NAMES AND ADDRESSES
Northwestern University Evanston Campus
Office for Sponsored Research (OSR)
1801 Maple Ave.
Evanston, IL 60201 -3149

8. PERFORMING ORGANIZATION REPORT NUMBER

9. SPONSORING/MONITORING AGENCY NAME(S) AND ADDRESS (ES)
U.S. Army Research Office
P.O. Box 12211
Research Triangle Park, NC 27709-2211

10. SPONSOR/MONITOR'S ACRONYM(S)
ARO

11. SPONSOR/MONITOR'S REPORT NUMBER(S)
63794-EG.4

12. DISTRIBUTION AVAILIBILITY STATEMENT
Approved for public release; distribution is unlimited.

13. SUPPLEMENTARY NOTES
The views, opinions and/or findings contained in this report are those of the author(s) and should not contrued as an official Department of the Army position, policy or decision, unless so designated by other documentation.

14. ABSTRACT
Mechanical properties of nanoscale free-standing polymer thin films exhibit size-dependence due to surface effects. However, it has remained a challenge to associate the length scales where such differences emerge with bulk polymer properties. Here we utilize molecular dynamics simulations to uncover the dependence of elastic modulus of free-standing films on film thickness and bulk properties. Comparison of glass transition temperature (Tg) and modulus (E) indicates that Tg converges to bulk value slightly faster as film thickness increases. The free surface effects that give rise to a depression in E and Tg are observed to be stronger for polymers with weaker

15. SUBJECT TERMS
elastic properties, thin film, polymer

16. SECURITY CLASSIFICATION OF:			17. LIMITATION OF ABSTRACT	15. NUMBER OF PAGES	19a. NAME OF RESPONSIBLE PERSON
a. REPORT	b. ABSTRACT	c. THIS PAGE			Sinan Keten
UU	UU	UU	UU		19b. TELEPHONE NUMBER 847-491-5282

Report Title

Size Dependent Mechanical Behavior of Free-Standing Glassy Polymer Thin Films

ABSTRACT

Mechanical properties of nanoscale free-standing polymer thin films exhibit size-dependence due to surface effects. However, it has remained a challenge to associate the length scales where such differences emerge with bulk polymer properties. Here we utilize molecular dynamics simulations to uncover the dependence of elastic modulus of free-standing films on film thickness and bulk properties. Comparison of glass transition temperature (Tg) and modulus (E) indicates that Tg converges to bulk value slightly faster as film thickness increases. The free surface effects that give rise to a depression in E and Tg are observed to be stronger for polymers with weaker intermolecular interactions. Our simulations suggest that the length scale of perturbation of free surface is only about several nanometers, but the effect is large enough that only films of 100 nm or larger exhibit negligible surface effects.

Size-Dependent Mechanical Behavior of Free-Standing Glassy Polymer Thin Films

Wenjie Xia[†] *and Sinan Keten*[*]

[†] Department of Civil & Environmental Engineering, Northwestern University, 2145 Sheridan Road, Evanston, IL 60208-3109. E-mail: *wenjiexia2011@u.northwestern.edu*

[*] Corresponding Author: Department. of Civil & Environmental Engineering and Department of Mechanical Engineering, Room A133, Northwestern University, 2145 Sheridan Road, Evanston, IL 60208-3109. Tel: 847-491-5282, E-mail: *s-keten@northwestern.edu*

KEYWORDS: elastic properties, film, polymer

ABSTRACT

Mechanical properties of nanoscale free-standing polymer thin films exhibit size-dependence due to surface effects. However, it has remained a challenge to associate the length scales where such differences emerge with bulk polymer properties. Here we utilize molecular dynamics simulations to uncover the dependence of elastic modulus (E) of free-standing films on film thickness and bulk properties. Comparison of glass transition temperature (T_g) and E indicates that T_g converges to bulk value slightly faster as film thickness increases. The free surface effects that give rise to a depression in E and T_g are observed to be stronger for polymers with weaker intermolecular interactions. The most intriguing aspect of our study is the finding that despite

the observed decrease in modulus of film up to a thickness over 100 nm, the local stress distribution reveals that the preserved length scale of perturbation of free surface is only about several nanometers. (*Abstract Figure: Fig. 1*)

INTRODUCTION

Ultra-thin polymer films with thickness in the range of tens of nanometers are becoming relevant for a wide array of applications in the field of nanotechnology and bioengineering, such as nanoelectronics [1], nanocomposites [2], coatings [3], polymeric membranes [4] and biosensors [5]. For instance, in nanoelectronics, the thermal and mechanical responses of nanopatterned polymeric structures obtained from lithography is important in determining the stability and reliability of these systems [6, 7]. In thin supported and free-standing films, the effects of free surfaces on the molecular structure and dynamics of polymer chains fundamentally changes the behaviors of these systems compared to bulk, and these effects become significantly more pronounced as the film thickness reaches below 100 nm. The free surface effects are complex and depend on many factors such as molecular weight of polymers, thickness of the film, and polymer chemistry, but a common observation is that the presence of surfaces in polymer thin films may result in a notable reduction of thermo-mechanical properties by shifting the relaxation time and enhancing the molecular mobility [8-12]. Understanding fundamental mechanisms pertaining to the thermo-mechanical properties, in particular, the glass transition temperature (T_g) and elastic modulus (E) of sub-100 nm polymer thin films are important for numerous technological applications of soft nanomaterials, and are being studied through novel experimental and computational techniques suited for the length scales of interest.

Previous studies have shown that intermolecular noncovalent weak interactions between polymer chains are crucial in determining thermo-mechanical responses of amorphous polymers. Experimental and theoretical studies have consistently shown that intermolecular forces between polymer chains can be tailored to tune T_g of bulk amorphous polymer [1, 13]. Concerning the mechanical behaviors, the investigations of energy partitioning have shown that the elastic modulus and yield response of amorphous polymer are mainly dominated by intermolecular noncovalent interactions (i.e. van der Waals interaction) [14, 15], and these mechanical properties are intimately related to segmental dynamics of chains and physical aging phenomena [16-19]. Low molecular weight plasticizing and antiplasticizing additives are often used to soften or stiffen polymer by changing their free volume and molecular packing [20, 21]. Experimental investigations and simulations have suggested that the interface and free surface effects on thermo-mechanical behaviors of polymer films can be influenced by numerous factors associated with intermolecular forces, such as retained solvents [22, 23], monomeric interactions [13, 24, 25] and chain-tacticity-related density variations [26, 27].

More recent efforts have been engaged in understanding the molecular origins of effects of free surfaces on thermo-mechanical properties of polymer films. The thickness-dependent behaviors of glass transition temperature and elastic modulus of polymer films have been characterized via experiments and simulations. Below T_g, the elastic moduli of polystyrene (PS) and poly(methyl methacrylate) (PMMA) films and nanostructures decrease dramatically below ~40 nm measured by a buckling-based metrology [28]. Torres et al. show that the T_g and elastic moduli of sub-100 nm methacrylate polymer films both decrease with film thickness, but the decrease in modulus of films is not correlated with the observed decrease in T_g [11]. A study by Declambre et al. shows that the elastic modulus of free-standing antiplasticized PMMA nanostructure decreases below

bulk value when the width is below 50 nm measured by beam bending deformation [29]. On the other hand, recent experimental evidences show surface stiffening as observed in polymer thin films in the rubbery regime above T_g [30-32], in which the underlying physics of mechanical behaviors could be fundamentally different from that below T_g.

However, due to the difficulty in measuring mechanical responses of polymer free-standing thin film with free surfaces only (no substrate) as illustrated in Figure 1 (a), current experimental techniques of measuring elastic modulus of film inevitably introduce substrate and retained solvents effects, which have been recently found to be crucial in determining the surface dynamics at nanoscale [33]. More importantly, how intermolecular forces between polymer chains interplay with free surface that changes influence in T_g and mechanical responses of polymer films remains challenging to discern, and the physics of this intriguing shift is yet to be fully explored. Nevertheless, direct comparison of polymers with different chemistry via experiments and all-atomistic simulations remains a challenge since these parameters cannot be continuously and independently varied. Simplified potentials in coarse-grained molecular dynamics (CGMD) simulations of free-standing film with free surfaces provide a clear benefit in this regard in addition to computational efficiency.

To facilitate a deeper understanding of the interplay between intermolecular forces and free surface effects on changing the thermo-mechanical responses of polymer thin films, we employ coarse-grained molecular dynamics simulations to investigate independent effects of these parameters. For this purpose, we establish a CGMD approach that builds on realistic parameters derived from all-atomistic MD simulation of PMMA. By employing this CG model as a starting point, we carry out large-scale MD simulations to assess the free surface effects by examining thickness-dependence behaviors of T_g and modulus of free-standing thin films with two free

surfaces. For modulus of polymer, we focus only on the elastic region at a glassy state below T_g, where polymers are deformed significantly faster than the intrinsic relaxation time and their mechanical properties are almost independent of temperature. The interplay between intermolecular forces and free surface effect on film T_g and modulus is evaluated by varying the depth of the effective weak interaction potential between monomers. The interfacial and characteristic length scales that correlate with the scales where T_g and E of thin film deviate from the bulk are examined and compared. A bilayer composite model derived from the spatial stress distribution is used to explain the physical origin of the size effect on film modulus.

METHODS

Coarse-grained Model Development

In order to simulate films with a characteristic dimension (i.e. thickness) reaching ~100 nm, we first present a coarse grained (CG) modeling approach based on the output of all-atomistic simulations of PMMA. The one bead per repeating unit mapping from the all-atomistic model to CG model and the resultant CG free-standing film configuration are illustrated in Figure 1 (b). The bonded interaction terms including the bond stretch and angle bending terms of the CG model are derived to match the corresponding probability distribution functions of all-atom model. For the intermolecular noncovalent interactions between chains (including interchain and intrachain interactions), we employ the truncated Lennard-Jones (LJ) 12-6 potential:

$$U_{LJ}(r) = 4\varepsilon\left[\left(\frac{\sigma}{r}\right)^{12} - \left(\frac{\sigma}{r}\right)^{6}\right] \qquad r < R_c \tag{1}$$

where ε is the depth of the potential well, and σ corresponds to the radial distance where the potential energy is zero. These two parameters are calibrated to match the experimental density at 300 K and T_g of bulk PMMA. The resultant values of σ and ε are 6.5 Å and 0.3 kcal/mol,

respectively, which yield a density of 1.17 g/cm^3 at 300 K and a bulk T_g of 388.6 K for our CG model. The cutoff distance of the intermolecular interaction R_c is chosen to be 15 Å. Detailed description of the coarse-graining strategy and simulation protocols can be found in our previous work [34].

Utilizing the atomistically informed CG model as the generic polymer model, we are able to explore the effect of intermolecular noncovalent interactions between chains on the thermo-mechanical properties (i.e. T_g and elastic modulus) of film systems with the existence of free surfaces at nanoscale. Taking the calibrated force-field parameters as a reference, we systematically vary ε from 0.2 to 0.4 kcal/mol to generate polymer models with different intermolecular interaction strength, while keeping σ the same and thus the density nearly constant for all simulations. It should be noted that once ε is varied, it is no longer representative of the original PMMA CG model. The similar two-bead type of CG models of methacrylate polymers has been recently reported [35]. Comparing with the two-bead models, the bonded interactions in our one-bead model preserve the general backbone features of methacrylate polymers, and the different values of ε can be a representative of different interactions resulting from the different type of side-chain groups. The simpler single bead model with less number of degree of freedom and atomic friction gives rise to overall softer mechanical responses than more realistic two-bead CG models and all-atomistic models [36], so the study here is meant to be largely comparative and qualitative.

Polymer Free-Standing Thin Film Configuration

CGMD free-standing thin film simulations are carried out using 50 to 500 chains with 100 repeat units per chain, resulting in thin films with thicknesses ranging from ~5 to ~90 nm (along the z axis). Periodic boundary conditions of the simulation box are applied in x-y plane with

dimensions of 9 nm × 9 nm except for ~5 nm thick films, in which we use larger dimensions of 18 nm × 18 nm in x-y plane to improve the sampling. The film thickness is estimated as the difference between the maximum and minimum z coordinate. In order to create two free surfaces of the film, the box dimension along the z-axis are taken to be larger than the film thickness and the boundary condition in that direction is nonperiodic. The initial film structures are built based on a self-avoiding random walk algorithm and placed at the center of the simulation box along the z-dimension. Then, the film first undergoes two annealing cycles from 550 K to 210 K and then equilibrated at 250 K for 2 ns under the isothermal-isobaric ensemble (NPT). The time step is chosen to be 4 fs.

Glass Transition Calculation

The calculations of glass transition temperatures of both bulk and film samples are carried out using the method described by Tsige and Taylor [37] from the measurement of mean-squared displacement (MSD) data of monomers in polymer chains. The MSD of polymer beads is evaluated as:

$$g_0(t) = \left\langle \left| r_i(t) - r_i(0) \right|^2 \right\rangle \tag{2}$$

where $r_i(t)$ is the position of the ith bead at time t and $\langle \dots \rangle$ denotes the ensemble averages. The time-averaged values of g_0 from 40 ps to 2000 ps are plotted against temperature from 490 K to 190 K at an interval of 20 K, which provides a metric of segmental mobility as a function of temperature. The MSD data in the lower temperature region and higher temperature region can be fitted with linear slopes, and the intersection of the two slopes marks the T_g.

Calculation of Elastic Modulus

To calculate the elastic modulus, strain-controlled uniaxial tensile deformation is simulated in the x direction (along the plane of the film), with a constant strain (engineering strain) rate of 0.5 ns^{-1}, while the pressure in the transverse direction (y) is controlled to be zero using the Nose-Hoover barostat. The z dimension of the simulation box is automatically adjusted to shrink and wrap to encompass all the beads during the simulations. The stress component in tensile direction is calculated based on the atomic virial stress tensor [38]:

$$\tau_{ij} = -\frac{1}{V}[\sum_{\alpha} m_{\alpha}(v_{\alpha})_i(v_{\alpha})_j - \sum_{\alpha>\beta}\frac{\partial U}{\partial r_{\alpha\beta}}\frac{(r_{\alpha\beta})_i(r_{\alpha\beta})_j}{r_{\alpha\beta}}] \quad (3)$$

where V is the volume of the actual polymer system instead of the simulation box, N is the total number of CG beads or monomers, and m_α and v_α denote the mass and velocity of αth monomer, respectively. The distance between the monomer pair α and β is denoted by $r_{\alpha\beta}$. U is the total potential energy including bond, angle and pair-wise nonbonded interactions. While the strain rate used in our study is higher than experimental studies, it is reasonably low for MD simulations, and the glassy modulus dependence on strain rate is relatively weaker than rubbery modulus measurements [39]. Thus, qualitatively, we don't anticipate strong rate dependence effects on the comparative analyses presented herein. The elastic modulus is measured as the slope from 0 to 4% strain over 10 replicas.

RESULTS AND DISCUSSION

We first characterize how T_g and elastic modulus E depend on the magnitude on the intermolecular interaction strength (ε) for bulk polymer systems (no free surfaces). The simulation results of bulk T_g and E are summarized in Table I. Both T_g and E systematically increase with ε. Recently, we have shown that increasing ε from 0.2 (soft) to 0.4 kcal/mol (hard) leads to a monotonic increase in bulk T_g [13], which can be ascribed to the fact that a stronger

intermolecular interaction leads to a greater activation energy barrier for polymer chains to achieve cooperative segmental motion. The result of uniaxial tensile tests for glassy bulk polymer at T = 250 K is shown in Figure 2. From the stress-strain responses, there is a distinct difference of deformation mechanisms between different ε values. For stronger intermolecular interaction ($\varepsilon = 0.4$ kcal/mol), four regimes can be observed: elastic, yield, strain softening and hardening regions. This is similar to experimental stress-strain observations on glassy polymers [39]. However, for weaker intermolecular interaction ($\varepsilon = 0.2$ kcal/mol), there is no obvious strain softening or hardening regime. The strain softening and hardening regimes with a stronger ε can be attributed to an increased activation energy associated with molecular arrangement and interchain sliding after elastic deformation [18]. For the elastic response, the bulk elastic modulus E increases with ε, which is consistent with previous findings, since the elastic work is primarily stored as non-bonded internal energy [14].

In polymer thin films, regions near free surfaces characterized by an enhanced mobility and a reduced density compared to interior bulk-like regions due to the less constraint on the surfaces are often called interfacial layers. The thickness of the interfacial layer, or the so-called interfacial thickness h^{int}, of a free-standing film is calculated on the basis of Gibbs dividing surface (GDS) concept in thermodynamics, which can be used as an indication of free surface effect on the mobility of polymer films. Figure 3 (a) shows the density profile along the z position of the film. The value of h^{int} is calculated by the equation: $h^{int} = (h_{max} - h_{eff})/2$, where h_{max} is the maximum film thickness defined by the distance between the maximum and minimum z coordinates of the film and h_{eff} is the effective thickness between the two GDS positions as labeled by the vertical dotted lines. Figure 3 (b) shows the result of h^{int} as a function of film thickness for different ε at 250 K (below bulk T_g). From the result, it can be

clearly observed that the polymer film with a lower value of ε has a larger h^{int} and thus a greater free surface effect on chain mobility for all the film thicknesses. The obtained interfacial thickness is about 0.5 to 1.0 nm, which is in the similar range as reported by earlier MD studies of polymer films [13, 40, 41]. For each ε, the film with different thickness exhibits almost the same value of h^{int}. By taking the mean value of h^{int} over different film thicknesses, we obtain the average interfacial thickness for each ε, which is listed in Table II.

The thickness dependence of T_g^{film} of free-standing films with different intermolecular interactions is shown in Figure 4. The behaviors that the T_g^{film} increases with film thickness and then converges to their bulk T_g are observed for all the ε values and comparable with experimental observations. The film exhibits a greater T_g^{film} over different thickness for a larger value of ε. However, for a polymer with a larger ε, the T_g^{film} converges to their bulk value faster with increasing thickness compared to a softer polymer with a lower ε. The free surface induced reduction in film T_g, which can be attributed to the enhanced mobile layer at a surface as discussed in earlier studies [42-45], is more significant for weaker intermolecular interaction. Therefore, the simulation result suggests that the free surface effect on the depression of film T_g is stronger for weaker intermolecular interaction.

To further quantify film thickness effects on T_g scaling and its relation to intermolecular interactions as shown in Figure 4, we employ the empirical fitting formula introduced by Kim et al. [46] to describe T_g^{film}:

$$T_g^{film}(h) = \frac{T_g^{bulk}}{1 + (\delta^T / h)} \tag{4}$$

where h is the film thickness, T_g^{bulk} is obtained from the bulk simulations (Table II), and δ^T is called the characteristic thickness that determines the saturation rate of T_g^{film} growth. The dashed lines in the plot represent the best fit of Eq. 4 to the data, and the obtained result of δ^T is summarized in Table II. By employing this simple empirical form that involves only one fitting parameter, we are able to more quantitatively assess how the relative free surface effects on the film change with different intermolecular forces. From Table II, it can be observed that the value of δ^T depends on the intermolecular interaction ε and it decreases with increasing ε, which is qualitatively consistent with h^{int} obtained from thermodynamic analysis of the film, even though the value of h^{int} is smaller than δ^T for each ε. This result indicates that the thermodynamic analysis of free surface (GDS) can be well correlated with the thickness dependence of film glass transition behavior, and suggests that both h^{int} and δ^T relate to the depth of the free surface layer with enhanced mobility for the systems studied herein.

Next, we measure the elastic modulus of free-standing films E^{film} with different ε, as well as different thickness values. Figure 5 (a) shows the snapshots of MD simulations during the tensile tests of the free-standing film. The thickness dependence of the modulus of the films E^{film} at 250 K is shown in Figure 5 (b). Similar to the glass transition behaviors of the films, the free surface induced decrease in E^{film} compared to the bulk value becomes more pronounced as the thickness decreases.

It appears from our results that both E^{film} and T_g^{film} are influenced by the presence of the free-surface effects in a free-standing thin films. This finding leads to the following question that we seek to answer here: does the characteristic length scale at which the deviation of E^{film} emerges from the bulk value correlates to that for the glass transition temperature?

As a first attempt to elucidate this issue, here we directly compare the free surface effects on the modulus and T_g of free-standing thin films by employing the functional form of Eq. 4 for both T_g^{film} and E^{film}. Specifically, we describe the thickness-dependence of film modulus as:

$$E^{film}(h) = \frac{E^{bulk}}{1 + (\delta^E / h)} \tag{5}$$

where δ^E is the characteristic thickness obtained from the modulus measurement. The best fit of Eq. 5 is denoted by the dotted lines in Figure 5 (b).

In essence, δ^E and δ^T can be considered as the comparable figures of merit that quantify the dependence of elastic modulus and glass-transition temperature on film thickness, which is directly related to length scale where film properties deviate from bulk values. The simulated values of δ^E as a function of intermolecular interaction strength are listed in Table II. The value of δ^E increases from 4 to 10 nm as ε decreases from 0.4 to 0.2 kcal/mol. This is reminiscent of the observation that the free surface effect on T_g is greater for lower ε. The values of δ^E are greater than those values of δ^T for the same ε, which indicates that the convergence of the modulus to the bulk value with an increase in the film thickness occurs more slowly compared with T_g^{film} as shown in Figure 5 (c).

Our observations over a broad parameter range hints towards a general applicability of some of the concepts arising from previous experimental studies. A study by Torres et al. [11] has shown that polymethacrylate films exhibit a much larger length scale for observed changes in the modulus at room temperature in comparison to their apparent T_g. Forrest et al. [47] also showed that the high-frequency mechanical properties of free-standing PS film measured by Brillouin light scattering (BLS) are not correlated with the film T_g as film thickness is varied. Wang and Mckenna [31] report that the significant T_g reduction for PS when the film thickness is less than 20

nm using the liquid dewetting method. Additionally, earlier studies by McKenna's group and others [32, 48, 49] have shown that the observed changes in rheological properties of polymer films with varying film thicknesses could not be well correlated with the T_g measurement.

To further interpret our results and quantify the length scale of perturbation of free surface, the information of distributions of the local stress and relaxation associated with segmental mobility of polymer chains within the film can provide insight into the nature of the surface effect. Figure 6 (a) shows the plot of both spatial distribution of local stress and segmental relaxation time as a function of film position z. The local stress $\tau(z) = \frac{1}{2}[\tau_{xx}(z) + \tau_{yy}(z)]$ is measured from the center to the free surface of the film intermediately after applying a biaxial step strain of 10% in x and y directions for ε = 0.2 kcal/mol. It can be clearly seen that the unrelaxed local stress is zero at the free surface boundary, and increases more or less linearly with the depth into the film, as labeled by the solid slope in the plot. At ~7 nm away from the free surface, the local stress saturates to the value in the interior region, which is indicated by the horizontal dashed line. Since at a constant strain, the stress developed will be related to the local modulus of the film, this analysis reveals that the free surface effect that gives rise to a linear gradient in the modulus that near surfaces can penetrate several nanometers into the film.

The local relaxation time τ_0 plotted in Figure 6 (a) can be defined as the time needed by the mean-squared displacement of CG beads within the local region to reach the bead size σ = 6.5 Å:

$$\boldsymbol{g_0(t = \tau_0, z) = \sigma} \tag{6}$$

Compared to the stress distribution, it can be observed that the length scale of the relaxation gradient within the surface region is slightly shorter than that of the stress gradient. Considering the fact that the film elastic modulus converges to the bulk value at a larger film thickness compared to T_g, this finding may suggest that length scales of film T_g and modulus do not have

to be exactly the same because the length scales of the gradient of the local stress and mobility in the surface region can be different. It should be noted that it is very challenging to accurately predict the spatial T_g within very small region less than ~1 nm using the current MSD approach. This is mainly because the segmental mobility of polymer chains can be very high and the monomers can diffuse out of the spatial region where they initially stay into other layers at a temperature close or above T_g. However, the local mobility via the measurement of local MSD should be related to T_g, since both properties are measured based on the information of segmental dynamics in our study.

On the basis of the local stress distribution across the film, we employ a composite bilayer model as illustrated in Figure 6 (b) to explain the thickness dependence of E^{film}. The film with a total thickness of h can be considered as a composite with two softer surface layers with a thickness of h^{surf} and one stiffer bulk-like interior region based on the spatial stress distribution. The shape of the profile in spatial stress is similar to that in density, but the values of h^{surf} is larger than the interfacial thickness h^{int} determined from GDS. Based on the observation that h^{int} is nearly independent of film thickness, one can assume that this linear gradient holds for different film thickness. Following this, the surface layer has an average modulus of $E^{surf} = E^{bulk}/2$. As the distance from the free surface increases beyond the linear gradient region, the free surface effect vanishes, and the modulus can be considered to be equal to E^{bulk}. If the film thickness h is less than $2h^{surf}$, this means that the effects of the two free surfaces are pervasive throughout the film and there is no interior bulk-like region. This approach is qualitatively similar to the concept of the glassy bridge reinforced model [50-52] that is introduced to explain the mechanical reinforcement of nanofilled elastomers. Then, E^{surf} becomes a linear function of h and is directly equal to E^{film}. Therefore, the E^{film} can be obtained based on the rule of mixtures:

$$E^{film} = \begin{cases} E^{bulk}\left(1 - \dfrac{h^{surf}}{h}\right) & h \geq 2h^{surf} \\ \dfrac{E^{bulk}}{4h^{surf}} h & h < 2h^{surf} \end{cases} \quad (7)$$

The prediction of Eq. 7 is represented by the solid curves in Figure 5 (b). For thinner films with thicknesses below ~10 nm, the prediction slightly underestimates the simulation results, which can be attributed to the less accuracy in the assumption of linear modulus gradient in the surface region when the film thickness is less or comparable to $2h^{surf}$. However, without any input fitting parameters, the behavior of the thickness dependence of E^{film} is well captured by the bilayer composite model. The values of h^{surf} determined from the local stress distribution increase with decreasing ε (Table II), which is consistent with our previous empirical scaling analysis using Eq. 5. Even though the values of h^{surf} arising from the stress perturbation of free surface are only in the range of 4 to 7 nm for different ε studied herein, the resultant change in modulus can be observed in a film with a thickness up to around 100 nm that is significantly larger compared to h^{surf}. These values are also comparable with experimental observations. In the previous experimental study [11], the thickness of the free-surface layer for PMMA films on PDMS is reported to be about 3.5 nm. Our simulation prediction of h^{surf} for ε = 0.4 kcal/mol is quite close to their value. In a recent study by Brinson et al. [53], they show that the interphase in the small local region near the substrate with a higher local modulus results in an altered elastic modulus of film up to hundreds of nanometers, which provides a support to our observation. In the simulations by Yoshimoto et al. [54], free-standing polymer film exhibits local softening regions with lower storage modulus at two free surfaces via the measurement of local dynamic mechanical properties, and the spatial modulus exhibits an nearly linear gradient in the surface region, which is very similar to what we observe herein. Therefore, our finding physically

explains why the E^{film} approaches to the bulk value as the film thickness increases by employing the bilayer composite model, and highlights the importance in determining the length scale of interphase region arising from free surfaces in polymer films.

CONCLUSION

In this study, we provide a comprehensive CGMD study that quantifies how the glass-transition temperature and elastic modulus at glassy state of free-standing polymer thin films depend on intermolecular interactions and film thickness. Both bulk and film systems exhibit a greater value of T_g and modulus with similar backbone structure but stronger intermolecular interaction. However, the free surface has a stronger effect on T_g and modulus for the film with a weaker intermolecular interaction at nanoscale. By comparing the results of T_g and modulus of the film, we find that the convergence of the modulus to the bulk value with an increase in the film thickness occurs more slowly compared with T_g. This longer-range free surface effect on modulus than T_g may be further supported by the observation of a greater length scale of local stress distribution in the surface region than that of local relaxation time. The observed decrease in modulus of film exists up to the thickness over ~100 nm. However, the measurement of local stress distribution induced by a step strain deformation reveals that there exists a soft region with a length scale on the order of several nanometers, which is much smaller than the critical film thickness where the film modulus converges to bulk value. The thickness dependence of film modulus is well captured by employing the concept of bilayer composite model, which physically explains why the modulus increases with film thickness. Our finding establishes a comprehensive description of free-standing film elastic properties, providing an analytical

description that highlights the importance in determining the length scale of interphase region arising from free surfaces in polymer thin films.

Tables

TABLE I. Comparison of glass-transition temperature (T_g) and elastic modulus (E) of bulk polymer at a glassy state (T = 250 K) for different intermolecular interaction strength (ε).

ε (kcal/mol)	T_g (K)	E (MPa)
0.2	321.5 ($\pm$18.7)	139.2 ($\pm$26.3)
0.3	388.6 ($\pm$10.1)	288.5 ($\pm$35.5)
0.4	411.1 ($\pm$21.7)	411.0 ($\pm$44.3)

TABLE II. Summary of different resultant surface related properties that are used to quantify the free surface effects and their relevant length scales as described in the text for different intermolecular interaction strength (ε).

ε (kcal/mol)	h^{int} (Å)	δ^T (nm)	δ^E (nm)	h^{surf} (nm)
0.2	8.6	3.2	10.3	7.0
0.3	6.9	2.1	6.6	5.0
0.4	5.7	1.0	4.2	4.0

Figures and Captions

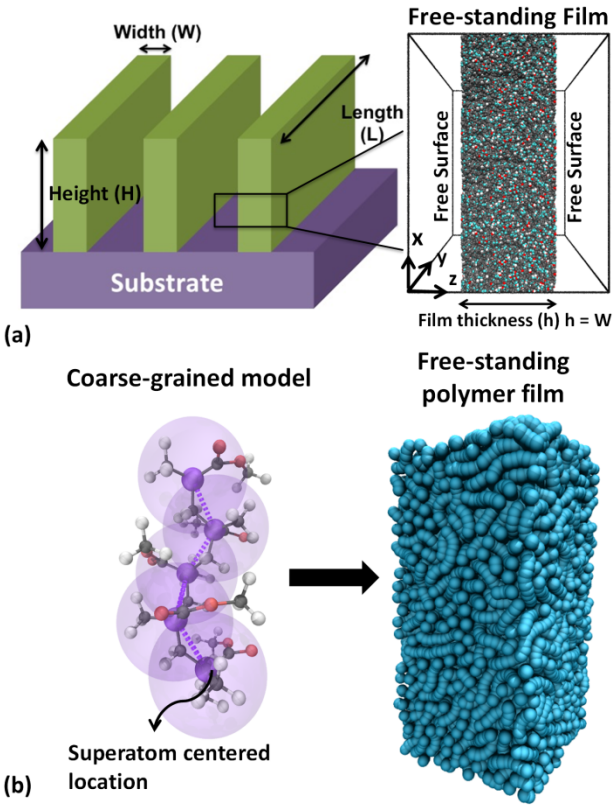

FIG. 1. (a) Illustration of polymer nanostructures with a width in nanoscale ($W \ll L, H$) (left) and the configuration of all-atomistic polymer free-standing film in simulations with periodic boundary conditions in x and y axis. (b) The mapping from the all-atom model of poly(methyl methacrylate) (PMMA) to the coarse-grained model (left) and the snapshot of the coarse-grained free-standing polymer film with two free surfaces on the top and bottom faces (right).

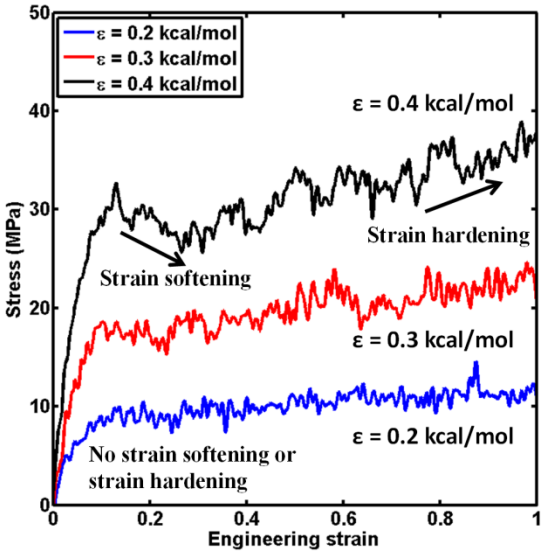

FIG. 2. Stress-strain response for bulk polymers with different intermolecular interactions (ε = 0.2, 0.3 and 0.4 kcal/mol) under uniaxial tension at 250 K. The elastic modulus is determined by fitting the data with the slope from 0 to 4% strain over 10 replicates.

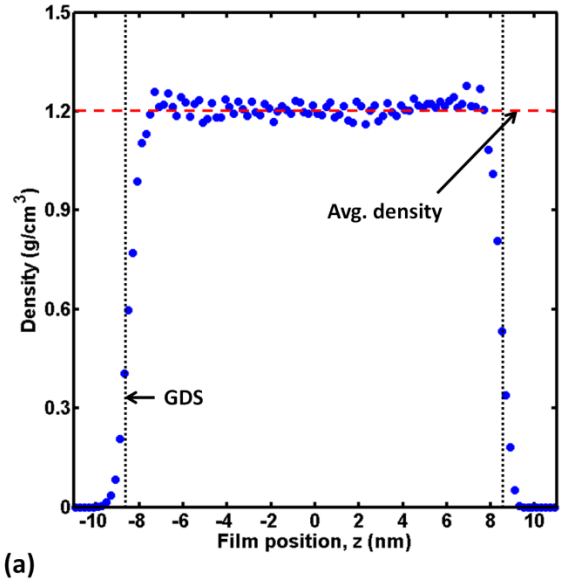

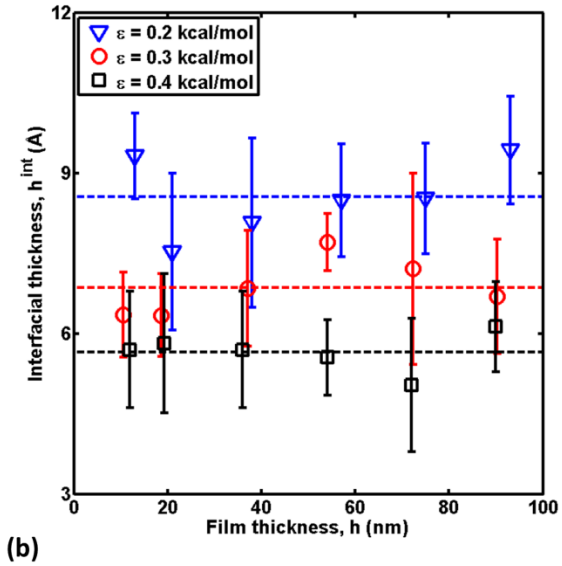

FIG. 3. (a) The density profile along the height of free-standing thin film (z) for ε = 0.3 kcal/mol at 250 K. **(b)** Interfacial thickness of mobile free surface layer h^{int} as a function of film thickness. The dashed lines indicate the mean value of h^{int} over different film thicknesses.

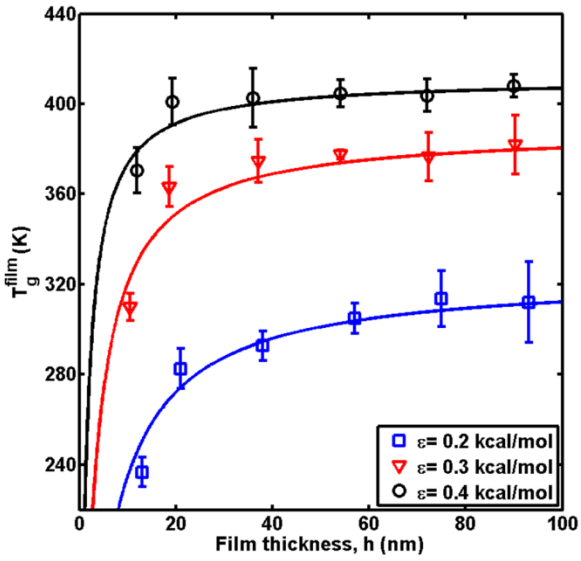

FIG. 4. The thickness dependence of the glass transition temperatures of free-standing thin film T_g^{film} for different ε. The solid line is calculated as the best fit of Eq. 4, which results in the fit parameter of the characteristic thickness δ^T for T_g^{film}.

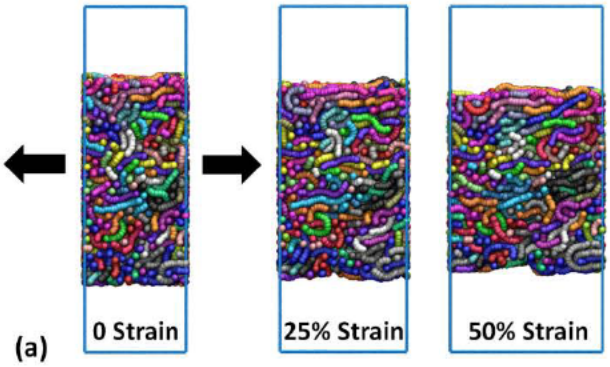
0 Strain
25% Strain
50% Strain

(a)

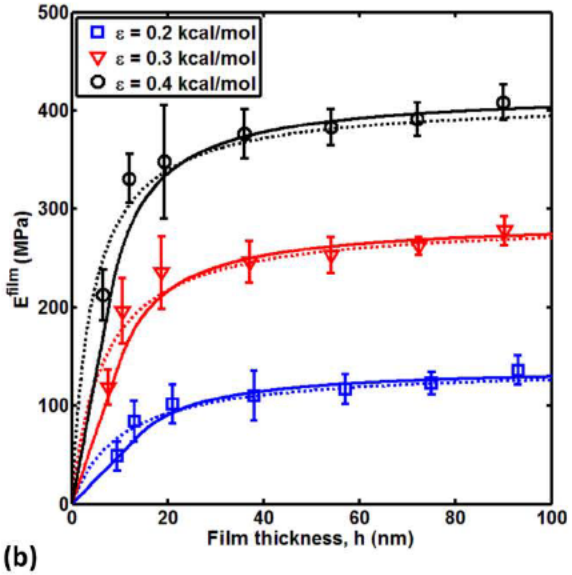
ε = 0.2 kcal/mol
ε = 0.3 kcal/mol
ε = 0.4 kcal/mol
E^film (MPa)
Film thickness, h (nm)

(b)

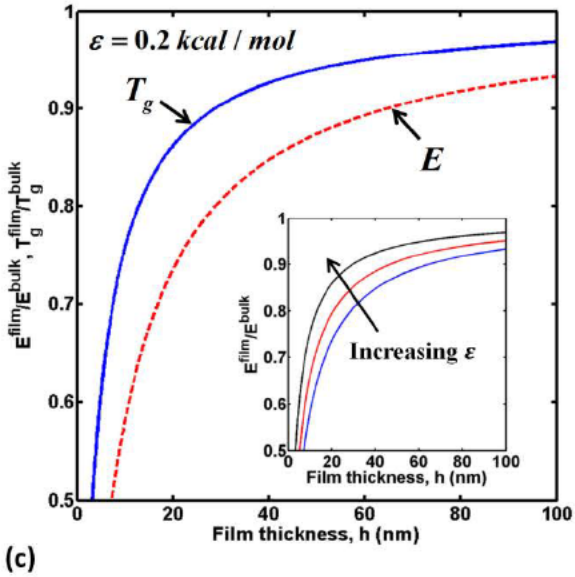
ε = 0.2 kcal / mol
T_g
E
Increasing ε
E^film/E^bulk, T_g^film/T_g^bulk
Film thickness, h (nm)

(c)

FIG. 5. (a) MD simulation snapshots during the tensile deformation of the free-standing film with a thickness of 18 nm. The arrows indicate the direction of deformation of the film. **(b)** The elastic modulus of free-standing film E^{film} as a function of film thickness for different ε. The dotted line is the fit of empirical scaling formula in Eq. 5. The solid line is prediction of Eq. 7 derived from the bilayer composite model. **(c)** Comparison of the empirical scaling results for the normalized T_g (T_g^{film}/T_g^{bulk}) and E $\left(E^{film}/E^{bulk}\right)$ as a function of film thickness. (Inset) Comparison of normalized E for different ε.

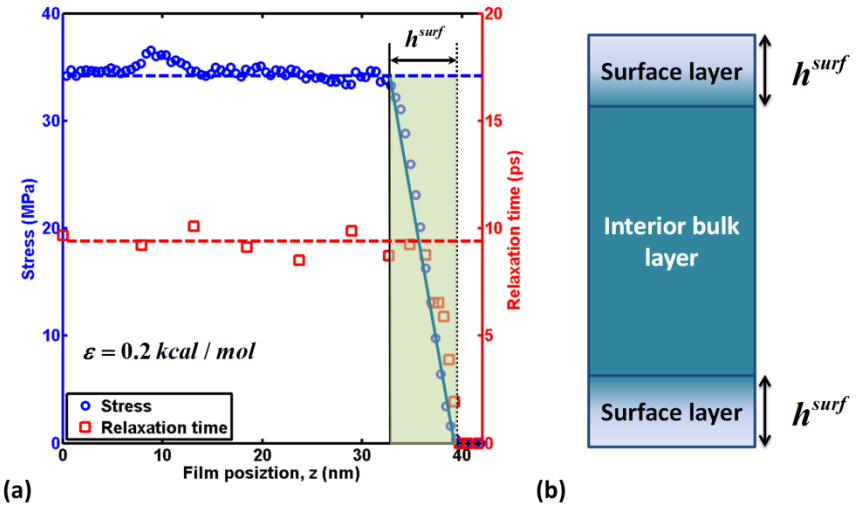

FIG. 6. (a) Spatial distributions of the stress and relaxation time across the film with a thickness of ~78 nm from the center to the free surface (ε = 0.2 kcal/mol). The local stress $\tau = \frac{1}{2}(\tau_{xx} + \tau_{yy})$ is measured in a biaxial deformation with a step strain of 10% in x and y directions. The local relaxation time is determined based on Eq. 6. The solid slope and dashed vertical lines correspond to the linear gradient of the stress within the surface layer and the average stress and relaxation time in the interior region of the film, respectively. The thickness of the surface layer h^{surf} is defined as the thickness of the linear slope region of the stress at the free surface labeled by the colored shadow in the plot. **(b)** The schematic of the bilayer composite model that consists

of two soft surface layers with a thickness of h^{surf} and an interior bulk-like layer derived from the local stress distribution.

ACKNOWLEDGMENTS

The authors acknowledge funding by the Army Research Office and Department of Civil & Environmental Engineering and Department of Mechanical Engineering at Northwestern University. A supercomputing grant from Quest HPC System at Northwestern University is acknowledged.

References

1. H. Ito: Chemical Amplification Resists for Microlithography, in Microlithography · Molecular Imprinting, (Springer, Heidelberg, Germany, 2005), pp. 37.
2. P.M. Ajayan, L.S. Schadler and P.V. Braun: Nanocomposite science and technology (Wiley, New York, USA, 2006).
3. P. Bertrand, A. Jonas, A. Laschewsky and R. Legras: Ultrathin polymer coatings by complexation of polyelectrolytes at interfaces: suitable materials, structure and properties. *Macromol. Rapid Comm.* **21**(7), 319 (2000).
4. B.W. Rowe, B.D. Freeman and D.R. Paul: Physical aging of ultrathin glassy polymer films tracked by gas permeability. *Polymer.* **50**(23), 5565 (2009).
5. J.R. Chen, Y.Q. Miao, N.Y. He, X.H. Wu and S.J. Li: Nanotechnology and biosensors. *Biotechnol. Adv.* **22**(7), 505 (2004).
6. K. Yoshimoto, M.P. Stoykovich, H.B. Cao, J.J. de Pablo, P.F. Nealey and W.J. Drugan: A two-dimensional model of the deformation of photoresist structures using elastoplastic polymer properties. *J. of Appl. Phys.* **96**(4), 1857 (2004).
7. A. Sharma and G. Reiter: Instability of thin polymer films on coated substrates: Rupture, dewetting, and drop formation. *J. Colloid Interface Sci.* **178**(2), 383 (1996).
8. C.B. Roth and J.R. Dutcher: Glass transition and chain mobility in thin polymer films. *J. Electroanal. Chem.* **584**(1), 13 (2005).
9. R.D. Priestley, C.J. Ellison, L.J. Broadbelt and J.M. Torkelson: Structural relaxation of polymer glasses at surfaces, interfaces and in between. *Science.* **309**(5733), 456 (2005).
10. J.A. Forrest and J. Mattsson: Reductions of the glass transition temperature in thin polymer films: probing the length scale of cooperative dynamics. *Phys. Rev. E.* **61**, R53 (2000).

11. J.M. Torres, C.M. Stafford and B.D. Vogt: Elastic Modulus of Amorphous Polymer Thin Films: Relationship to the Glass Transition Temperature. *ACS Nano.* **3**(9), 2677 (2009).

12. P.Z. Hanakata, J.F. Douglas and F.W. Starr: Interfacial mobility scale determines the scale of collective motion and relaxation rate in polymer films. *Nat. Commun.* **5**, 4163 (2014).

13. W. Xia and S. Keten: Coupled Effects of Substrate Adhesion and Intermolecular Forces on Polymer Thin Film Glass-Transition Behavior. *Langmuir.* **29**(41), 12730 (2013).

14. D. Hossain, M.A. Tschopp, D.K. Ward, J.L. Bouvard, P. Wang and M.F. Horstemeyer: Molecular dynamics simulations of deformation mechanisms of amorphous polyethylene. *Polymer.* **51**(25), 6071 (2010).

15. J. Li, T. Mulder, B. Vorselaars, A.V. Lyulin and M.A.J. Michels: Monte Carlo Simulation of Uniaxial Tension of an Amorphous Polyethylene-like Polymer Glass. *Macromolecules.* **39**(22), 7774 (2006).

16. A.V. Lyulin, N.K. Balabaev, M.A. Mazo and M.A.J. Michels: Molecular Dynamics Simulation of Uniaxial Deformation of Glassy Amorphous Atactic Polystyrene. *Macromolecules.* **37**(23), 8785 (2004).

17. L.A.G. Gray and C.B. Roth: Stability of polymer glasses vitrified under stress. *Soft Matter.* **10**(10), 1572 (2014).

18. R. Jörg: Fracture in glassy polymers: a molecular modeling perspective. *J. Phys.: Condens. Matter.* **21**(46), 463101 (2009).

19. D. Hudzinskyy, M.A.J. Michels and A.V. Lyulin: Mechanical properties and local mobility of atactic-polystyrene films under constant-shear deformation. *J. of Chem. Phys.* **137**(12), (2012).

20. R.F. Landel and L.E. Nielsen: Mechanical properties of polymers and composites, 2nd ed. (CRC Press, New York, USA, 1993).

21. R.A. Riggleman, J.F. Douglas and J.J. de Pablo: Antiplasticization and the elastic properties of glass-forming polymer liquids. *Soft Matter.* **6**(2), 292 (2010).

22. S. Kim, M.K. Mundra, C.B. Roth and J.M. Torkelson: Suppression of the Tg-Nanoconfinement Effect in Thin Poly(vinyl acetate) Films by Sorbed Water. *Macromolecules.* **43**(11), 5158 (2010).

23. J.M. Torres, C.M. Stafford and B.D. Vogt: Manipulation of the Elastic Modulus of Polymers at the Nanoscale: Influence of UV−Ozone Cross-Linking and Plasticizer. *ACS Nano.* **4**(9), 5357 (2010).

24. C.J. Ellison, M.K. Mundra and J.M. Torkelson: Impacts of Polystyrene Molecular Weight and Modification to the Repeat Unit Structure on the Glass Transition−Nanoconfinement Effect and the Cooperativity Length Scale. *Macromolecules.* **38**(5), 1767 (2005).

25. W. Xia, D.D. Hsu and S. Keten: Dependence of Polymer Thin Film Adhesion Energy on Cohesive Interactions between Chains. *Macromolecules.* (2014).

26. Y. Grohens, M. Brogly, C. Labbe, M.-O. David and J. Schultz: Glass Transition of Stereoregular Poly(methyl methacrylate) at Interfaces. *Langmuir.* **14**(11), 2929 (1998).

27. Y. Grohens, L. Hamon, G. Reiter, A. Soldera and Y. Holl: Some relevant parameters affecting the glass transition of supported ultra-thin polymer films. *Eur. Phys. J. E.* **8**(2), 217 (2002).

28. C.M. Stafford, B.D. Vogt, C. Harrison, D. Julthongpiput and R. Huang: Elastic Moduli of Ultrathin Amorphous Polymer Films. *Macromolecules.* **39**(15), 5095 (2006).

29. S.P. Delcambre, R.A. Riggleman, J.J. de Pablo and P.F. Nealey: Mechanical properties of antiplasticized polymer nanostructures. *Soft Matter.* **6**(11), 2475 (2010).

30. P.A. O'Connell and G.B. McKenna: Dramatic stiffening of ultrathin polymer films in the rubbery regime. *Eur. Phys. J. E.* **20**(2), 143 (2006).

31. J. Wang and G.B. McKenna: Viscoelastic and Glass Transition Properties of Ultrathin Polystyrene Films by Dewetting from Liquid Glycerol. *Macromolecules.* **46**(6), 2485 (2013).

31. P.A. O'Connell and G.B. McKenna: Rheological Measurements of the Thermoviscoelastic Response of Ultrathin Polymer Films. *Science.* **307**(5716), 1760 (2005).

32. C.M. Evans, S. Narayanan, Z. Jiang and J.M. Torkelson: Modulus, Confinement, and Temperature Effects on Surface Capillary Wave Dynamics in Bilayer Polymer Films Near the Glass Transition. *Phys. Rev. Lett.* **109**(3), 038302 (2012).

33. W. Xia, S. Mishra and S. Keten: Substrate vs. free surface: Competing effects on the glass transition of polymer thin films. *Polymer.* **54**(21), 5942 (2013).

34. D.D. Hsu, W. Xia, S.G. Arturo and S. Keten: Systematic Method for Thermomechanically Consistent Coarse-Graining: A Universal Model for Methacrylate-Based Polymers. *J. Chem. Theory Comput.* ***10****(6), 2514* (2014).

35. T.W. Rosch, J.K. Brennan, S. Izvekov and J.W. Andzelm: Exploring the ability of a multiscale coarse-grained potential to describe the stress-strain response of glassy polystyrene. *Phys. Rev. E.* **87**(4), 042606 (2013).

37. M. Tsige and P.L. Taylor: Simulation study of the glass transition temperature in poly(methyl methacrylate). *Phys. Rev. E.* **65**(2), 021805 (2002).

38. M.P. Allen and D.J. Tildesley: Computer simulation of liquids (Oxford university press, New York, USA, 1989).

39. A.D. Mulliken and M.C. Boyce: Mechanics of the rate-dependent elastic–plastic deformation of glassy polymers from low to high strain rates. *Int. J. Solids Struct.* **43**(5), 1331 (2006).

40. C. Li and A. Strachan: Effect of Thickness on the Thermo-Mechanical Response of Free-Standing Thermoset Nanofilms from Molecular Dynamics. *Macromolecules.* **44**(23), 9448 (2011).

41. W.M. Huang, B. Yang, L. An, C. Li and Y.S. Chan: Water-driven programmable polyurethane shape memory polymer: Demonstration and mechanism. *Appl. Phys. Lett.* **86**(11), (2005).

42. J.S. Sharp, J.H. Teichroeb and J.A. Forrest: The properties of free polymer surfaces and their influence on the glass transition temperature of thin polystyrene films. *Eur. Phys. J. E.* **15**(4), 473 (2004).

43. J.S. Sharp and J.A. Forrest: Free surfaces cause reductions in the glass transition temperature of thin polystyrene films. *Phys. Rev. Lett.* **91**(23), 235701 (2003).

44. J. Mattsson, J.A. Forrest and L. Borjesson: Quantifying glass transition behavior in ultrathin free-standing polymer films. *Phys. Rev. E.* **62**(4), 5187 (2000).

45. J.L. Keddie, R.A.L. Jones and R.A. Cory: Size-Dependent Depression of the Glass-Transition Temperature in Polymer-Films. *Europhys. Lett.* **27**(1), 59 (1994).

46. J.H. Kim, J. Jang and W.-C. Zin: Estimation of the Thickness Dependence of the Glass Transition Temperature in Various Thin Polymer Films. *Langmuir.* **16**(9), 4064 (2000).

47. J.A. Forrest, K. Dalnoki-Veress and J.R. Dutcher: Brillouin light scattering studies of the mechanical properties of thin freely standing polystyrene films. *Phys. Rev. E.* **58**(5), 6109 (1998).

48. H. Bodiguel and C. Fretigny: Reduced Viscosity in Thin Polymer Films. *Phys. Rev. Lett.* **97**(26), 266105 (2006).

49. S.A. Hutcheson and G.B. McKenna: Nanosphere Embedding into Polymer Surfaces: A Viscoelastic Contact Mechanics Analysis. *Phys. Rev. Lett.* **94**(7), 076103 (2005).

50. S. Merabia, P. Sotta and D.R. Long: A Microscopic Model for the Reinforcement and the Nonlinear Behavior of Filled Elastomers and Thermoplastic Elastomers (Payne and Mullins Effects). *Macromolecules.* **41**(21), 8252 (2008).

51. D. Long and P. Sotta: Nonlinear and Plastic Behavior of Soft Thermoplastic and Filled Elastomers Studied by Dissipative Particle Dynamics. *Macromolecules.* **39**(18), 6282 (2006).

52. A. Papon, S. Merabia, L. Guy, F. Lequeux, H. Montes, P. Sotta and D.R. Long: Unique Nonlinear Behavior of Nano-Filled Elastomers: From the Onset of Strain Softening to Large Amplitude Shear Deformations. *Macromolecules.* **45**(6), 2891 (2012).

51. S. Watcharotone, C.D. Wood, R. Friedrich, X. Chen, R. Qiao, K. Putz and L.C. Brinson: Interfacial and Substrate Effects on Local Elastic Properties of Polymers Using Coupled Experiments and Modeling of Nanoindentation. *Adv. Eng. Mater.* **13**(5), 400 (2011).

52. K. Yoshimoto, T.S. Jain, P.F. Nealey and J.J. de Pablo: Local dynamic mechanical properties in model free-standing polymer thin films. *J. Chem. Phys.* **122**(14), 144712 (2005).